AV-1451 Tau and β-Amyloid Positron Emission Tomography Imaging in Dementia With Lewy Bodies

Kejal Kantarci, MD, MS,[1] Val J. Lowe, MD,[1] Bradley F. Boeve, MD,[2] Matthew L. Senjem, MS,[1,3] Nikki Tosakulwong, BS,[4] Timothy G. Lesnick, MS,[4] Anthony J. Spychalla, BS,[1] Jeffrey L. Gunter, PhD,[1,3] Julie A. Fields, PhD,[5] Jonathan Graff-Radford, MD,[2] Tanis J. Ferman, PhD,[6] David T. Jones, MD,[2] Melissa E. Murray, PhD,[7] David S. Knopman, MD,[2] Clifford R. Jack, Jr., MD,[1] and Ronald C. Petersen, MD, PhD[2,4]

Objective: Patients with probable dementia with Lewy bodies (DLB) often have Alzheimer's disease (AD)-related pathology. Our objective was to determine the pattern of positron emission tomography (PET) tau tracer AV-1451 uptake in patients with probable DLB, compared to AD, and its relationship to β-amyloid deposition on PET.
Methods: Consecutive patients with clinically probable DLB (n = 19) from the Mayo Clinic Alzheimer's Disease Research Center underwent magnetic resonance imaging, AV-1451, and Pittsburgh compound-B (PiB) PET examinations. Age- and sex-matched groups of AD dementia (n = 19) patients and clinically normal controls (n = 95) from an epidemiological cohort served as a comparison groups. Atlas- and voxel-based analyses were performed.
Results: The AD dementia group had significantly higher AV-1451 uptake than the probable DLB group, and medial temporal uptake completely distinguished AD dementia from probable DLB. Patients with probable DLB had greater AV-1451 uptake in the posterior temporoparietal and occipital cortex compared to clinically normal controls, and in probable DLB, the uptake in these regions correlated with global cortical PiB uptake (Spearman rho = 0.63; $p = 0.006$).
Interpretation: Medial temporal lobe AV-1451 uptake distinguishes AD dementia from probable DLB, which may be useful for differential diagnosis. Elevated posterior temporoparietal and occipital AV-1451 uptake in probable DLB and its association with global cortical PiB uptake suggest an atypical pattern of tau deposition in DLB.

ANN NEUROL 2017;81:58–67

Patients who meet clinical criteria for probable dementia with Lewy bodies (DLB) may have overlapping Lewy body disease and Alzheimer's disease (AD)-related pathology. Because of this overlap, the pathological classification of DLB is made by taking into account both the extent of Lewy body disease and AD-related pathologies. Whereas amyloid positron emission tomography (PET) imaging demonstrates high β-amyloid (Aβ) pathology in more than half of the patients with probable DLB,[1] the data on the presence and distribution of tau pathology in probable DLB is limited to autopsy studies. Autopsy data are usually obtained during the end stages of the disease process and typically involves selective regional sampling of the brain. PET imaging of tau pathology with AV-1451 or other tau tracers would improve our understanding of the regional distribution of tau pathology and its

This article was published online on 19 December 2016. After online publication, the Acknowledgments were revised. This notice is included in the online and print versions to indicate that both have been corrected on 12 January 2017.

View this article online at wileyonlinelibrary.com. DOI: 10.1002/ana.24825

Received Aug 15, 2016, and in revised form Nov 7, 2016. Accepted for publication Nov 7, 2016.

Address correspondence to Dr Kejal Kantarci, Department of Radiology, Mayo Clinic, 200 First Street Southwest, Rochester, MN 55905. E-mail: kantarci.kejal@mayo.edu

From the [1]Department of Radiology, Mayo Clinic, Rochester, MN; [2]Department of Neurology, Mayo Clinic, Rochester, MN; [3]Department of Information Technology, Mayo Clinic, Rochester, MN; [4]Department of Health Sciences Research, Mayo Clinic, Rochester, MN; [5]Department of Psychiatry and Psychology, Mayo Clinic, Rochester, MN; [6]Department of Psychiatry and Psychology, Mayo Clinic, Jacksonville, FL; and [7]Department of Laboratory Medicine and Pathology, Mayo Clinic, Jacksonville, FL

influence on clinical disease severity in patients with probable DLB.[2,3]

AV-1451 binds to AD-related tau pathology with high affinity.[4,5] Within the spectrum of preclinical AD, mild cognitive impairment attributed to AD, and AD dementia, the pattern of AV-1451 binding is consistent with the Braak staging of the neurofibrillary tangle pathology of AD in a majority of the cases.[6–10] However, the pattern and magnitude of AV-1451 binding may show variability in AD,[8] and this variation has been associated with both age at onset[11] and variability in disease symptoms.[12] The regional distribution of AV-1451 binding in probable DLB patients has been studied in a limited number of cases.[13] Early evidence suggests that AV-1451 binding corresponds well to immunoreactive AD-related tau pathology, with no evidence for binding to α-synuclein neuropathology in either multiple system atrophy or Lewy body disease cases.[4,5]

The first objective of this study was to determine the regional pattern of AV-1451 binding in a cohort of patients with probable DLB compared to patients with AD dementia and clinically normal controls (CN). The second objective was to assess the potential relationship between AV-1451 binding with disease duration, dementia severity, and with the global cortical Aβ deposition measured with ^{11}C Pittsburgh compound-B (PiB) PET in probable DLB.

Patients and Methods

Subjects

Consecutive patients who fulfilled the 3rd Consortium Criteria for probable DLB were recruited to a multimodal neuroimaging study conducted at the Mayo Clinic Alzheimer's Disease Research Center (ADRC) from May 2015 through September 2016. All patients who fulfilled the clinical criteria for probable DLB[14] were invited to participate in magnetic resonance imaging (MRI), AV-1451 PET, and PiB PET studies within 3 months of the clinical evaluation. All probable DLB participants (n = 19) underwent MRI and AV-1451 PET examinations, and with the exception of 1 patient, all participated in PiB PET studies.

For comparison, we included an equal number of AD dementia patients with high uptake on PiB PET (n = 19) from the Mayo Clinic ADRC who were evaluated during the same time period with the same multimodality neuroimaging protocol and who were of a similar age and sex to the DLB participants. The diagnosis of AD dementia was made based on the National Institute on Aging–Alzheimer's Association Criteria.[15] We also included a clinically normal control group (CN; n = 95) of similar age and sex to the probable DLB participants from the Mayo Clinic Study of Aging, which is a population-based study on aging.[16] To be included as a control, the participants had to have low uptake on PiB PET scans.

Participants were excluded if they had neurological conditions that may have interfered with cognitive function or brain imaging findings, such as traumatic brain injury, intracranial tumor, large hemispheric infarct, epilepsy, or normal pressure hydrocephalus. None of the probable DLB patients who agreed to participate in this study had these comorbidities.

Quantitative measures of dementia severity were obtained using cognitive (Mini–Mental State Examination [MMSE] and Mattis Dementia Rating Scale [DRS]) and noncognitive functional assessment (Clinical Dementia Rating Scale [CDR]; presence of parkinsonism was recorded, and the degree of extrapyramidal motor impairment was assessed through the Unified Parkinson's Disease Rating Scale part III [UPDRS-III]). Visual hallucinations were characterized by being fully formed, not restricted to a single episode, and not related to another medical issue, treatment, or advanced dementia. Fluctuations were considered to be present if the patients scored 3 to 4 on the four-item Mayo Fluctuations Scale.[17] Probable rapid eye movement sleep behavior disorder (RBD) was defined as previously published.[18] Informants and patients were interviewed regarding temporal onset of disease signs and symptoms.

The Mayo Clinic Institutional Review Board approved this study. All subjects and, when appropriate, a surrogate provided written informed consent before participating in any research activity.

MRI and PET Acquisitions

MRI examinations were performed at 3 Tesla (GE Healthcare, Milwaukee, WI). A three-dimensional (3D) high-resolution magnetization prepared rapid gradient echo acquisition with approximately 1-mm cubic resolution was obtained for anatomical segmentation and labeling.

A PET/computed tomography scanner (DRX; GE Healthcare) operating in 3D mode was used to acquire PET images. Patients were injected with an average of 596MBq (range, 292–729) of ^{11}C-PiB and an average of 370MBq (range, 333–407) of ^{18}F-AV1451. Following a 40-minute ^{11}C-PiB uptake period, a 20-minute PiB scan consisting of four 5-minute dynamic frames was obtained. A 20-minute AV-1451 PET scan was obtained after 80 minutes of uptake.

AV-1451 and PiB PET Image Analysis

PET image analysis was performed using an automated image processing pipeline, which included registration of the PET image volumes to each subject's own T_1-weighted MRI for the segmentation of gray and white matter, as previously described.[19] Regional cortical uptake of AV-1451 and PiB was determined from an in-house modified version of the Automated Anatomical Labeling atlas, as previously described.[20] Fraction of tissue and cerebrospinal fluid (CSF) compartments in each AV-1451 PET voxel were derived from the registered T_1-weighted MRI. Correction for partial volume averaging of CSF was applied using the two-compartment model in each AV-1451 PET voxel.[21] In a supplementary analysis, partial volume correction was not applied to AV-1451 PET. The global cortical PiB retention standardized uptake value ratio (SUVr) was

TABLE. Characteristics of Participants

	Control (N = 90)	AD (N = 18)	DLB (N = 15)	p^*
Male, n (%)	90 (95)	18 (95)	18 (95)	>0.99
Age, years	67 (7)	69 (8)	67 (7)	0.51
Education, years	15 (2)	15 (3)	16 (3)	0.60
APOE ε4 carrier, n (%)	19 (20)	14 (93)	5 (33)	0.002
PiB SUVr	1.29 (0.05)	2.52 (0.45)	1.56 (0.40)	<0.001
MMSE		19 (8)	24 (5)	0.047
CDR-SOB score		5.5 (3.5)	6.0 (3.3)	0.68
CDR Global score		0.9 (0.5)	0.9 (0.6)	0.84
Dementia Rating Scale Total Score		118.6 (16.3)	115.2 (31.4)	0.71
UPDRS-III		0 (1)	12 (8)	<0.001
Cognitive impairment Duration, years		5.3 (2.2)	7.2 (5.7)	0.22
Visual hallucinations, No. (%) Duration, years			6 (33) 4.5 (2.7)	
Fluctuations, No. (%) Duration, years			14 (82) 4.5(3.9)	
Parkinsonism, No. (%) Duration, years			17 (94) 4.5 (3.9)	
RBD, present No. (%) Duration, years			17 (94) 8.3 (5.0)	

Unless indicated otherwise, data shown are mean (standard deviation).

* p values were assessed using Fisher's exact test, Student t test, or analysis of variance.

APOE ε4 = apolipoprotein E ε4; PiB = Pittsburgh compound-B; SUVr = standardized uptake value ratio; MMSE = Mini–Mental State Examination; CDR = Clinical Dementia Rating Scale; CDR-SOB = CDR Sum of Boxes; UPDRS-III = Unified Parkinson's Disease Rating Scale part III; RBD = rapid eye movement sleep behavior disorder; AD = Alzheimer's disease; DLB = dementia with Lewy bodies.

obtained from the bilateral parietal (including posterior cingulate and precuneus), temporal, prefrontal, orbitofrontal, and anterior cingulate regions referenced to the cerebellum region, as previously described.[19] A PiB PET SUVr of >1.42 was considered to be high uptake on PiB PET scans.

AV-1451 uptake in each voxel was referenced to the median value of the right and left cerebellar crus uptake. An exploratory voxel-based analysis (voxel-based morphometric; VBM) was conducted in SPM comparing the DLB group to both the CN and AD groups. Maps of these comparisons are displayed at the $p < 0.001$ level. Correction for multiple comparisons was applied using family-wise error correction. If a comparison did not show any findings after the correction, we carried out an uncorrected analysis, not to miss any important findings in this exploratory analysis. Median AV-1451 SUVr from the right and left hemispheric regions of interest (ROIs) were calculated.

Statistical Analysis

Subject characteristics were compared among the clinical groups with the Fisher's exact test, Student t test, or analysis of variance, followed by Tukey's honest significant differences test for pair-wise comparisons. Area under the receiver operating characteristic curves (AUROCs) were calculated for distinguishing DLB and CN, and DLB and AD groups using the median AV-1451 SUVr of each atlas ROI after combining the left and right hemispheric ROIs. Because we were conducting comparisons in 46 different ROIs, we adjusted for multiple comparisons using a Bonferroni correction to control the family-wise error rate. A value of $p < 0.05$ was considered statistically significant after Bonferroni correction was applied. Correlations of AV-1451 SUVr from the atlas meta-ROIs with global cortical PiB SUVr, measures of disease severity, and duration of symptoms were described and tested with Spearman rank correlations in the probable DLB group.

Results

The three clinical groups, AD dementia, probable DLB, and CN, were similar in age and had a median age (range) of 67 (55–81) years. Except for 1 woman, all probable DLB patients were men; therefore, the comparison groups (probable AD and CN) were also primarily composed of men. The probable AD group had a higher frequency of *APOE* ε4 carriers compared to both probable DLB and CN groups ($p = 0.002$). Measures of functional (CDR Sum of Boxes; CDR-SOB), and cognitive (DRS) disease severity were not different between the

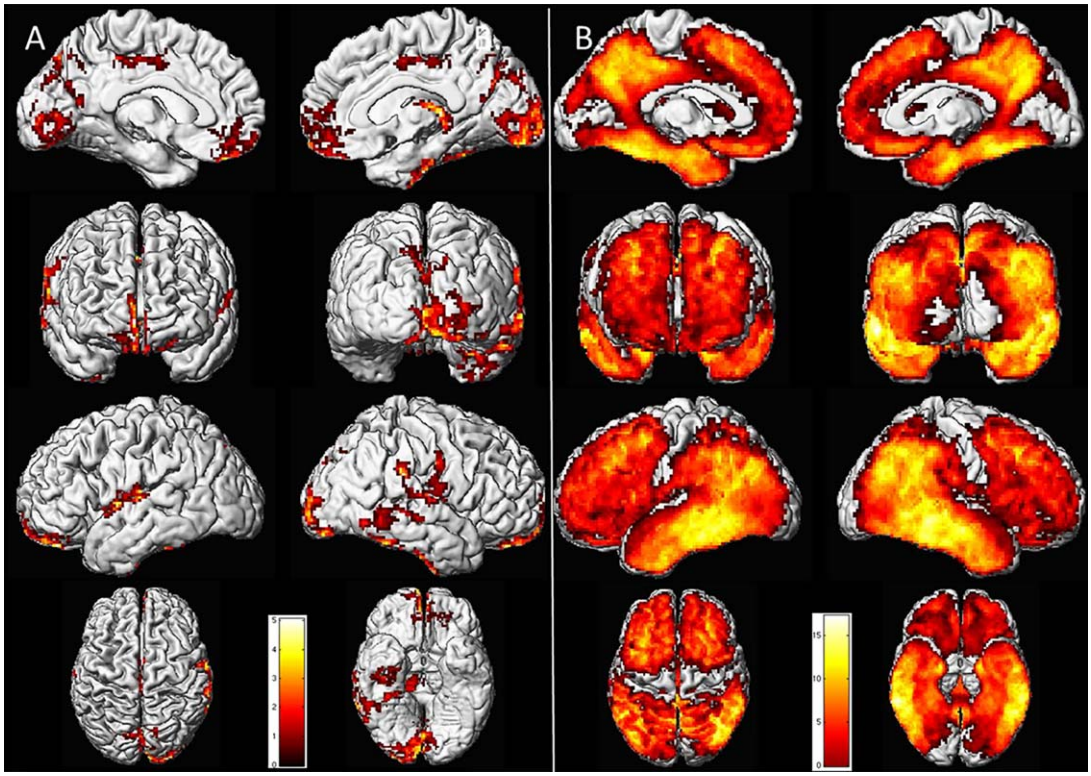

FIGURE 1: Regional pattern of AV-1451 uptake in probable DLB patients compared to the clinically normal controls and probable AD dementia. Voxel-based analysis comparing patients with probable DLB to the clinically normal control group indicate greater uptake in the posterior and inferior temporoparietal lobes and medial frontal cortex in probable DLB patients compared to controls. Higher uptake in the choroid plexus is seen on the left side ($p < 0.001$; uncorrected for multiple comparisons). Correction for multiple comparisons revealed no findings. (A) Voxel-based analysis comparing patients with probable DLB to AD dementia showed significant differences throughout the brain relatively sparing the somatosensory and primary visual cortices ($p < 0.001$; family-wise error corrected for multiple comparisons). (B) Color bars show the t-value range. AD = Alzheimer's disease; DLB = dementia with Lewy bodies.

AD dementia and DLB groups; however, probable DLB patients had higher parkinsonism severity (UPDRS-III), but lower MMSE, scores compared to AD dementia patients. Whereas parkinsonism, fluctuations and probable RBD was present in a majority of the probable DLB patients (82–94%), visual hallucinations were less common (33%). Global cortical PiB SUVr was higher in probable DLB patients compared to CN and higher in probable AD dementia patients compared to both probable DLB and CN (Table).

The exploratory VBM analysis comparing the DLB and CN groups did not show any differences in AV-1451 binding after family-wise error correction for multiple comparisons. However, an uncorrected analysis revealed greater uptake in the inferior and lateral temporal and occipital cortex as well as the precuneus and cingulate regions in probable DLB patients compared to CN ($p < 0.001$). We did not observe higher AV-1451 binding in any region in the CN group compared to the DLB patients in both the family-wise error corrected and uncorrected comparisons ($p > 0.001$). AD dementia patients had higher AV-1451 binding in almost all regions of the brain, relatively sparing the inferior and medial occipital cortex, and somatosensory cortex compared to DLB patients after family-wise error correction for multiple comparisons ($p < 0.001$). Highest t values were observed in the temporal and parietal lobes. We did not observe higher AV-1451 binding in any region in the DLB group compared to the AD dementia patients in both the family-wise error corrected and uncorrected comparisons ($p > 0.001$; Fig 1).

The 46 atlas ROIs were ranked according to the area under the receiver operating characteristic curve (AUROC) for distinguishing DLB from CN (Fig 2A). AV-1451 SUVr was higher in a number of ROIs in the DLB group compared to the CN group; however, after applying Bonferroni correction for multiple comparisons, the following cortical regions had greater AV-1451 SUVr in probable DLB patients compared to the control group: inferior, middle, and superior occipital, lingual, angular, fusiform, middle and inferior temporal gyri, and precuneus and cuneus. Therefore, we combined these regions into one posterior temporoparietal and occipital meta-ROI for further investigation. There were no ROIs

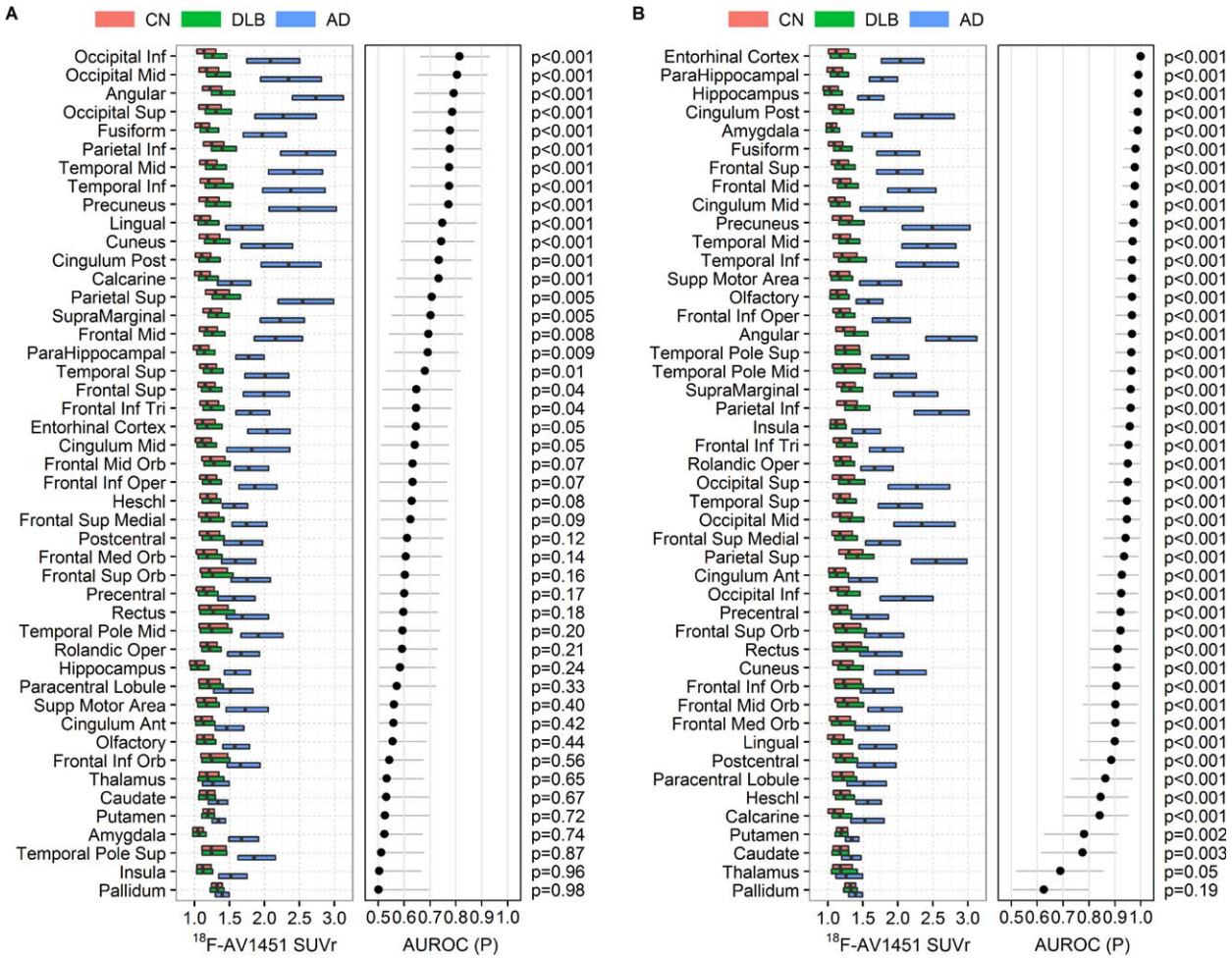

FIGURE 2: AV-1451 uptake in individual ROIs in patients with probable DLB compared to controls and patients with AD dementia. Median AV-1451 SUVr from the atlas ROIs and the interquartile ranges are presented with box plots in the three groups. ROIs are ordered according to the area under the receiver operating characteristic curve (AUROC) from highest to lowest with confidence intervals and the *p* value of the difference between the probable DLB and control (A); probable DLB and AD dementia (B) groups. AD = Alzheimer's disease; CN = clinically normal controls; DLB = dementia with Lewy bodies; ROIs = regions of interest; SUVr = standard value uptake unit ratio.

that had higher AV-1451 SUVr in the CN group compared to the DLB group (Fig 3A).

Except for the pallidum and thalamus, all ROIs showed higher AV-1451 SUVr in the AD group compared to the DLB group (Fig 2B). After applying Bonferroni correction for multiple comparisons, all ROIs except the caudate, pallidum, thalamus, and putamen significantly distinguished AD and DLB groups. Among those, the parahippocampal gyrus, entorhinal cortex, and hippocampus had an AUROC >0.99. Therefore, we combined these regions into one medial temporal meta-ROI for further investigation. When combined, the AV-1451 SUVr in these regions completely distinguished AD and DLB groups. The lowest medial temporal AV-1451 SUVr value observed in the AD group was 1.38, and the highest value observed in the probable DLB group was 1.33. (Fig 3B) There were no ROIs that had higher AV-1451 SUVr in the DLB group compared to the AD group.

There were 8 probable DLB patients who had high uptake on PiB PET (median global cortical SUVr [range] = 1.86 [1.44, 2.47]). The remaining 10 probable DLB patients had low PiB PET uptake (global cortical SUVr, < 1.42). All 8 of these cases had the posterior temporoparietal and occipital meta-ROI AV-1451 SUVr at or above the median value (1.28) within the DLB group. There were 4 additional probable DLB patients with posterior temporoparietal and occipital meta-ROI AV-1451 SUVr at or above the median value in the DLB group, but they did not have elevated PiB uptake (PiB SUVr, < 1.42). Two DLB cases with PiB and AV-1451 scans are presented in Figure 4. The posterior temporoparietal and occipital meta-ROI AV-1451 SUVr correlated with the global cortical PiB SUVr in patients with probable DLB (Spearman rho = 0.63; $p = 0.006$; Fig 5). The correlation between the medial temporal meta-ROI AV-1451 SUVr and the global cortical PiB SUVr showed a similar trend, but did not

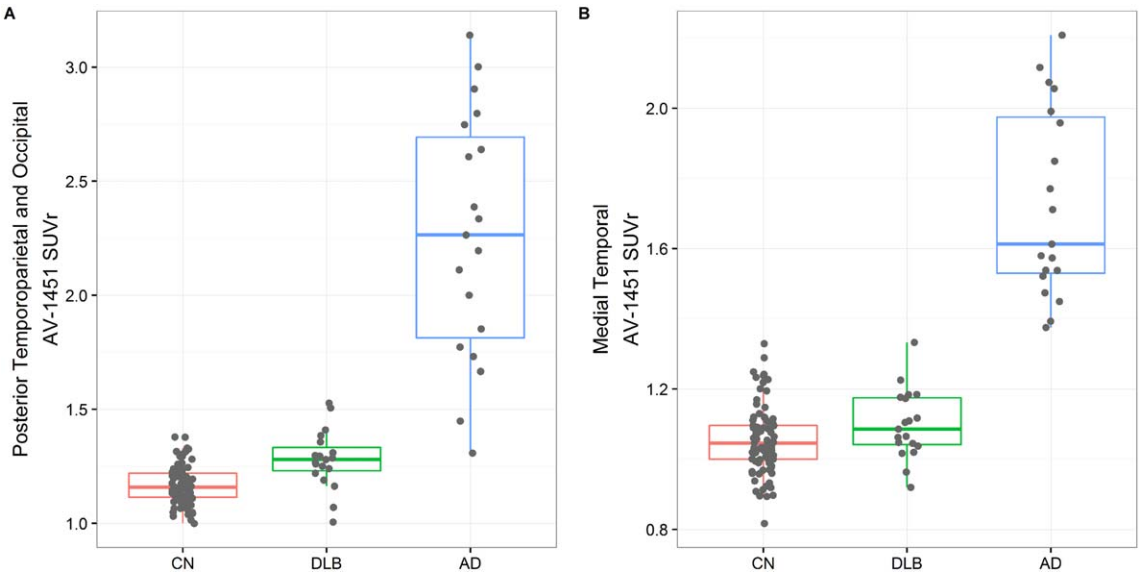

FIGURE 3: Box plots show the AV-1451 SUVr values in each subject from the posterior temporoparietal and occipital lobe meta-ROI (inferior, middle and superior occipital, lingual, angular, fusiform, middle and inferior temporal gyri, and precuneus and cuneus ROIs) (A) and the medial temporal lobe meta-ROI (parahippocampal gyrus, entorhinal cortex, and hippocampus) (B). AD = Alzheimer's disease; CN = clinically normal controls; DLB = dementia with Lewy bodies; ROI = region of interest; SUVr = standard value uptake unit ratio.

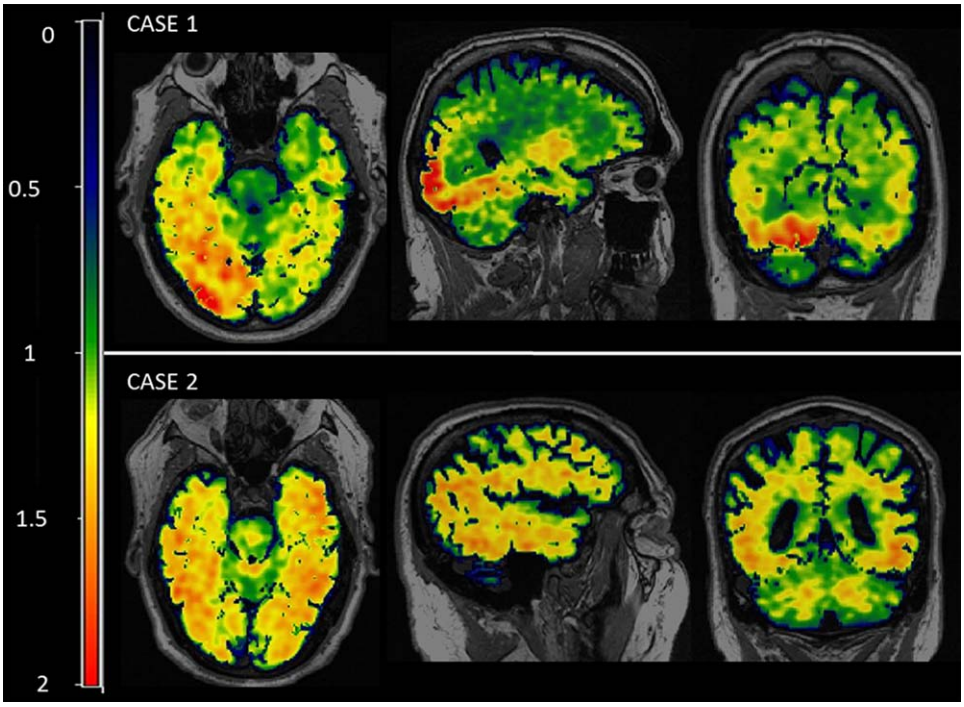

FIGURE 4: AV-1451 uptake in probable DLB patients with high and low uptake on PiB PET scans. AV-1451 PET scans are registered to T_1-weighted MRI. Each AV-1451 PET voxel was referenced to the median value of the right and left cerebellar crus uptake. The color scale in the AV-1451 PET images indicates a range of standard value uptake unit ratio (SUVr) in each PET voxel. Case 1 is a 65-year-old man with parkinsonism, fluctuations, probable rapid eye movement sleep behavior disorder (RBD), and a disease duration of 6.6 years. He has high uptake on the PiB PET scan with a global cortical SUVr of 1.71. There is significant AV-1451 uptake in the right inferior occipital lobe and moderate uptake in the inferior temporal lobes. Case 2 is a 78-year-old man with parkinsonism, fluctuations, probable RBD, and a disease duration of 5.0 years. He has low uptake on PiB PET scan, with a global cortical SUVr of 1.30. There is moderate AV-1451 uptake in the inferior temporal and occipital lobes. DLB = dementia with Lewy bodies; MRI = magnetic resonance imaging; PET = positron emission tomography; PiB = Pittsburgh compound-B.

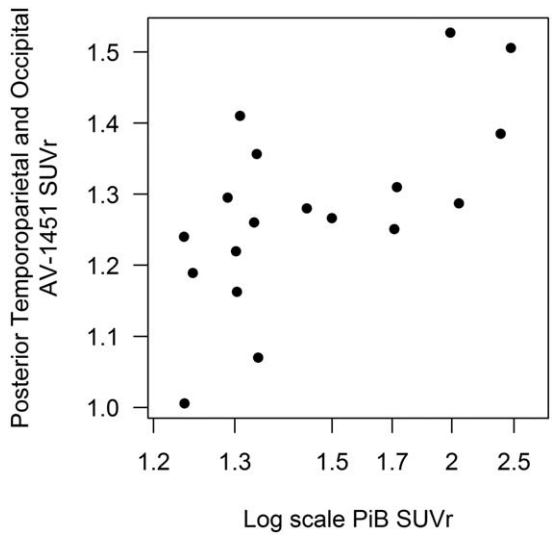

FIGURE 5: Correlations between AV-1451 SUVr in the posterior temporoparietal and occipital meta-ROI and global cortical PiB SUVr in patients with probable DLB (n = 18; because 1 DLB patient did not have PiB PET). The global cortical PiB SUVr is scaled with log transformation attributed to the skewing at lower SUVr levels (Spearman rho = 0.63; $p = 0.006$). DLB = dementia with Lewy bodies; PET = positron emission tomography; PiB = Pittsburgh compound-B; SUVr = standard value uptake unit ratio.

reach statistical significance in patients with probable DLB (Spearman rho = 0.40; $p = 0.10$).

We did not find an association between the posterior temporoparietal and occipital meta-ROI AV-1451 SUVr and the disease duration, CDR-SOB, DRS, MMSE, UPDRS-III, duration of visual hallucinations, fluctuations, parkinsonism, and RBD in patients with probable DLB ($p > 0.05$).

In a supplemental analysis, we investigated findings without partial volume correction. The findings did not change without the partial volume correction, but the AUROC values for distinguishing groups were lower and the correlation coefficients were weaker compared to the partial volume corrected data.

Discussion

We found significantly lower AV-1451 uptake in clinically probable DLB compared to patients with AD dementia. In particular, greater AV-1451 uptake in the medial temporal meta-ROI distinguished AD dementia from probable DLB. Patients with probable DLB had greater AV-1451 uptake in the posterior and inferior temporoparietal and occipital lobes compared to the control group of similar age and sex and low global cortical PiB SUVr (<1.4). Higher AV-1451 uptake in the posterior temporoparietal and occipital meta-ROI correlated with higher global cortical PiB SUVr in probable DLB.

Autoradiographic analyses on histopathological specimens indicate that AV-1451 is a potential surrogate marker for paired helical-filament-tau in AD.[4,5,22] Accordingly, patients with probable AD in the current study had significantly higher AV-1451 than those with probable DLB in almost all brain regions, with relative sparing of the primary cortices (ie, primary visual and somatosensory cortices). AV-1451 uptake in the medial temporal meta-ROI, including the entorhinal cortex, parahippocampal gyrus, and hippocampus, was entirely consistent with the clinical diagnoses of probable DLB and AD dementia. Preservation of medial temporal lobe structures is a supportive feature for the clinical diagnosis of probable DLB.[14] Medial temporal lobe atrophy is associated with the Braak stage of neurofibrillary tangle pathology and tau density in this region in patients with Lewy body disease pathology.[23–26] However, this feature has been criticized for its limited specificity, with medial temporal lobe atrophy also occurring in cases with hippocampal sclerosis, frontotemporal lobar degeneration, and argyrophilic grains disease.[27] Therefore, it is expected that higher AV-1451 uptake would be a more-specific marker for the presence of AD-related tau pathology in this region. Relative sparing of the primary somatosensory and the visual cortices may be expected given that these primary cortices get involved with the tau pathology during the latest stages of AD.[28]

Compared to clinically normal controls, patients with probable DLB had elevated AV-1451 uptake in the posterior and inferior temporoparietal regions, with greatest uptake observed in the occipital lobe visual association cortices. The distribution of the AV-1451 uptake in probable DLB was different from the expected distribution of AV-1451 uptake according to the Braak neurofibrillary tangle staging.[28] Therefore, it is important to determine whether this pattern of AV-1451 uptake truly represents hyperphosphorylated tau pathology in probable DLB. In an autopsy cohort of clinically diagnosed probable DLB patients, who had various loads of hyperphosphorylated tau and α-synuclein pathologies, the greatest load of hyperphosphorylated tau was found in the occipital lobes followed by the temporal lobes. Some of the lowest amount of hyperphosphorylated tau in patients with probable DLB was found in the hippocampus, which distinguished probable DLB cases from those with AD dementia.[29] Our findings in patients with probable DLB fully agree with these observations in autopsied cases, suggesting that the distribution of tau pathology in probable DLB follows an atypical pattern when compared to patients with typical AD dementia who tend to follow the Braak staging of the neurofibrillary tangle pathology of AD.[28]

In a smaller sample of probable DLB patients (n = 7) than those in the current study, abnormal AV-1451 in probable DLB was localized to the inferolateral temporal and parietal/precuneus regions.[13] Although we also found greater AV-1451 uptake in these regions in patients with probable DLB compared to the CN group, the inferior and middle occipital lobe was affected more than the inferior temporal and precuneus regions. The differences in findings may be attributed to differences in sample size and power, as well as the differences in the probable DLB and control groups that were studied. The control group used in the earlier study had approximately equal proportion of women and men, whereas the DLB group was predominantly men. In the current study, the control and probable DLB groups were fully matched on sex, and therefore the differences we found among the clinical groups were not influenced by sex differences. Furthermore, the probable DLB patients in the current study had lower UPDRS-III scores pointing to milder parkinsonism than the probable DLB patients included in the earlier study.

In DLB, progression of α-synuclein pathology in the neocortex is thought to begin in the inferior temporal and occipitotemporal regions,[30] which is consistent with fluorodeoxyglucose PET imaging studies that show greatest metabolic reductions in the posterior temporoparietal and occipital lobes.[31] In addition, tau deposition in DLB occurs in regions also affected by α-synuclein,[32] with evidence of tau and α-synuclein coaggregation in the same neuronal populations.[33] Differences in the local interaction between tau and different "strains" of α-synuclein has been observed in cell-to-cell transmission models,[34] with early evidence that tau and one possible strain of α-synuclein interacting by coseeding and promoting each other's aggregation.[34–36] In a recent pathological analysis of DLB, regional neocortical distribution of tau and α-synuclein density was greatest in the inferior temporal and occipitotemporal cortices.[37] The possibility that AV-1451 uptake in patients with probable DLB may be associated with coseeding of tau and α-synuclein in the neocortex is intriguing and worthy of further study.

All probable DLB patients with high amyloid load on PiB PET had high AV-1451 uptake in the posterior temporoparietal and occipital lobes. The cutpoint of PiB SUVR of 1.42 was chosen for low or high amyloid load based on the reliable worsening cut-point method,[38] which also correspond to approximately Thal phase 2 amyloid pathology.[39] Above this cutpoint, the PiB SUVr tends to increase over time, distinguishing older CN cases who are on a path to increasing amyloid deposition. However, we note that even cases with PiB SUVR of <1.42 may have some amyloid pathology and possibly tau pathology, which may influence AV-1451 findings when comparing DLB patients to CN, particularly in the entorhinal cortex.[6–10] To the extent that AV-1451 is a surrogate for the AD-related tau pathology in DLB, the probable DLB patients with high PiB and AV-1451 uptake likely have a mixture of AD and Lewy body disease pathologies. Although the correlation between the cortical PiB and AV-1451 uptake in the posterior temporoparietal and occipital cortex suggest that this atypical pattern of AV-1451 uptake in DLB patients is associated with AD-related pathology, there were a few DLB patients with elevated AV-1451 uptake in the posterior temporoparietal and occipital cortex, who had a low uptake on the PiB PET scan. It is possible that tau deposition may be followed by increased Aβ levels, and probable DLB patients with elevated AV-1451 uptake in the posterior temporoparietal and occipital cortex may develop Aβ pathology in the future. Indeed, there is a relationship between greater amyloid deposition and higher atrophy rates in the temporal and occipital lobes in patients with probable DLB,[40] and increased cortical atrophy in DLB is associated with presence of additional AD-related pathology[41] and Braak staging of neurofibrillary tangle tau pathology in autopsy-confirmed DLB.[42] Longitudinal studies may clarify the temporal relationship between increased AV-1451 uptake in the posterior temporoparietal and occipital cortex and amyloid deposition in DLB.

This study had a number of limitations related to the relatively small sample size. First, although we recruited consecutive patients with probable DLB to our cohort, almost all of the cases were men, with only 1 woman. Probable DLB is more common in men than women, with up to 4-fold higher incidence rate in men compared to women.[43] Nonetheless, sex differences in the extent and regional distribution of tau pathology may be present in patients with probable DLB. Second, it was not possible to investigate the relationship between AV-1451 uptake in probable DLB patients with and without each of the clinical features, and, in particular, we were unable to examine the relationship between occipital AV-1451 uptake and visual hallucinations attributed to limited number of cases with this disease feature. Visual hallucinations are known to be associated with hypometabolism in the occipital lobe,[44,45] and the relationship between visual hallucinations and occipital AV-1451 uptake is of interest. When duration of these symptoms was investigated in a subset of probable DLB patients with parkinsonism, fluctuations, and RBD, no association with posterior temporoparietal and occipital AV-1451 uptake was observed. Neither did we find an association between posterior temporoparietal and

occipital AV-1451 uptake and continuous measures of disease severity, such as DRS, MMSE, CDR-SOB, and UPDRS-III. In this cohort of mild-to-moderately demented patients with probable DLB, the effect of AV-1451 uptake on disease severity was negligible. However, it is possible that increased posterior temporoparietal and occipital AV-1451 uptake would have an impact on disease progression and survival. Faster disease progression has been observed in probable DLB patients with higher amyloid load on PiB PET[40] and hippocampal atrophy on MRI.[46]

In conclusion, AV-1451 uptake and, particularly, uptake in the medial temporal lobe fully distinguished AD dementia from probable DLB. This is in line with the current pathological criteria indicating that the likelihood of clinical expression of DLB is higher when Lewy body disease is present with neurofibrillary tangles at low Braak stages.[47,48] This concordance between the AV-1451 uptake and clinical disease expression indicates that AV-1451 uptake may be a valid marker for the tau neurofibrillary tangle stage in DLB patients with mixed AD and Lewy body disease pathologies. Medial temporal lobe AV-1451 uptake has important implications for improving the specificity of the clinical criteria for DLB and identifying probable DLB patients with AD-related tau pathology who may benefit from tau-modifying therapies. The atypical AV-1451 uptake in the occipital cortex needs further investigation with autopsy confirmation of tau deposition in this region in patients with probable DLB.

Acknowledgments

This study was funded by the NIH (R01 AG040042, R01 AG11378, P50 AG16574, U01 AG06786, and C06 RR018898), Foundation Dr. Corinne Schulerand, the Mangurian Foundation for Lewy Body Research, The Elsie and Marvin Dekelboum Family Foundation, and the Robert H. and Clarice Smith and Abigail Van Buren Alzheimer's Disease Research Program.

We would like to thank AVID Radiopharmaceuticals, Inc., for their support in supplying AV-1451 precursor, chemistry production advice and oversight, and FDA regulatory cross-filing permission and documentation needed for this work.

Author Contributions

K.K., N.T., and T.G.L. contributed to study concept and design. K.K., V.J.L., B.F.B., M.L.S., N.T., T.G.L., A.J.S., J.L.G., J.A.F., J.G.R., T.J.F., D.T.J., M.E.M., D.S.K., C.R.J, and R.C.P. contributed to acquisition of data, analysis, and interpretation of the data. K.K., N.T., and A.J.S. contributed to drafting the manuscript and figures. All authors reviewed the manuscript and approved the final version of the manuscript.

Potential Conflicts of Interest

Nothing to report.

References

1. Petrou M, Dwamena BA, Foerster BR, et al. Amyloid deposition in Parkinson's disease and cognitive impairment: a systematic review. Mov Disord 2015;30:928–935.
2. Gomperts SN, Marquie M, Locascio JJ, et al. PET radioligands reveal the basis of dementia in Parkinson's disease and dementia with Lewy bodies. Neurodegener Dis 2016;16:118–124.
3. Dani M, Brooks DJ, Edison P. Tau imaging in neurodegenerative diseases. Eur J Nucl Med Mol Imaging 2016;43:1139–1150.
4. Lowe VJ, Curran G, Fang P, et al. An autoradiographic evaluation of AV-1451 Tau PET in dementia. Acta Neuropathol Commun 2016;4:58.
5. Marquie M, Normandin MD, Vanderburg CR, et al. Validating novel tau positron emission tomography tracer [F-18]-AV-1451 (T807) on postmortem brain tissue. Ann Neurol 2015;78:787–800.
6. Johnson KA, Schultz A, Betensky RA, et al. Tau positron emission tomographic imaging in aging and early Alzheimer disease. Ann Neurol 2016;79:110–119.
7. Schwarz AJ, Yu P, Miller BB, et al. Regional profiles of the candidate tau PET ligand 18F-AV-1451 recapitulate key features of Braak histopathological stages. Brain 2016;139(pt 5):1539–1550.
8. Scholl M, Lockhart SN, Schonhaut DR, et al. PET imaging of tau deposition in the aging human brain. Neuron 2016;89:971–982.
9. Wang L, Benzinger TL, Su Y, et al. Evaluation of tau imaging in staging Alzheimer disease and revealing interactions between beta-amyloid and tauopathy. JAMA Neurol 2016;73:1070–1077.
10. Cho H, Choi JY, Hwang MS, et al. In vivo cortical spreading pattern of tau and amyloid in the Alzheimer disease spectrum. Ann Neurol 2016;80:247–258.
11. Cho H, Choi JY, Hwang MS, et al. Tau PET in Alzheimer disease and mild cognitive impairment. Neurology 2016;87:375–383.
12. Ossenkoppele R, Schonhaut DR, Scholl M, et al. Tau PET patterns mirror clinical and neuroanatomical variability in Alzheimer's disease. Brain 2016;139(pt 5):1551–1567.
13. Gomperts SN, Locascio JJ, Makaretz SJ, et al. Tau positron emission tomographic imaging in the Lewy body diseases. JAMA Neurol 2016;73:1334–1341.
14. McKeith IG, Dickson DW, Lowe J, et al. Diagnosis and management of dementia with Lewy bodies: third report of the DLB Consortium. Neurology 2005;65:1863–1872.
15. McKhann GM, Knopman DS, Chertkow H, et al. The diagnosis of dementia due to Alzheimer's disease: recommendations from the National Institute on Aging-Alzheimer's Association workgroups on diagnostic guidelines for Alzheimer's disease. Alzheimers Dement 2011;7:263–269.
16. Roberts RO, Geda YE, Knopman DS, et al. The Mayo Clinic Study of Aging: design and sampling, participation, baseline measures and sample characteristics. Neuroepidemiology 2008;30:58–69.
17. Ferman TJ, Smith GE, Boeve BF, et al. DLB fluctuations: specific features that reliably differentiate DLB from AD and normal aging. Neurology 2004;62:181–187.
18. Boeve BF, Molano JR, Ferman TJ, et al. Validation of the Mayo Sleep Questionnaire to screen for REM sleep behavior disorder in an aging and dementia cohort. Sleep Med 2011;12:445–453.

19. Jack CR, Jr., Lowe VJ, Senjem ML, et al. 11C PiB and structural MRI provide complementary information in imaging of Alzheimer's disease and amnestic mild cognitive impairment. Brain 2008; 131(pt 3):665–680.
20. Vemuri P, Gunter JL, Senjem ML, et al. Alzheimer's disease diagnosis in individual subjects using structural MR images: validation studies. NeuroImage 2008;39:1186–1197.
21. Lowe VJ, Kemp BJ, Jack CR, Jr., et al. Comparison of 18F-FDG and PiB PET in cognitive impairment. J Nucl Med 2009;50:878–886.
22. Sander K, Lashley T, Gami P, et al. Characterization of tau positron emission tomography tracer [18F]AV-1451 binding to postmortem tissue in Alzheimer's disease, primary tauopathies, and other dementias. Alzheimers Dement 2016;12:1116–1124.
23. Murray ME, Ferman TJ, Boeve BF, et al. MRI and pathology of REM sleep behavior disorder in dementia with Lewy bodies. Neurology 2013;81:1681–1689.
24. Burton EJ, Mukaetova-Ladinska EB, Perry RH, et al. Neuropathological correlates of volumetric MRI in autopsy-confirmed Lewy body dementia. Neurobiol Aging 2012;33:1228–1236.
25. Burton EJ, Barber R, Mukaetova-Ladinska EB, et al. Medial temporal lobe atrophy on MRI differentiates Alzheimer's disease from dementia with Lewy bodies and vascular cognitive impairment: a prospective study with pathological verification of diagnosis. Brain 2009;132(pt 1):195–203.
26. Kantarci K, Ferman TJ, Boeve BF, et al. Focal atrophy on MRI and neuropathologic classification of dementia with Lewy bodies. Neurology 2012;79:553–560.
27. Walker Z, Possin KL, Boeve BF, Aarsland D. Lewy body dementias. Lancet 2015;386:1683–1697.
28. Braak H, Braak E. Neuropathological stageing of Alzheimer-related changes. Acta Neuropathol 1991;82:239–259.
29. Walker L, McAleese KE, Thomas AJ, et al. Neuropathologically mixed Alzheimer's and Lewy body disease: burden of pathological protein aggregates differs between clinical phenotypes. Acta Neuropathol 2015;129:729–748.
30. Braak H, Ghebremedhin E, Rub U, Bratzke H, Del Tredici K. Stages in the development of Parkinson's disease-related pathology. Cell Tissue Res 2004;318:121–134.
31. Minoshima S, Foster NL, Sima AA, et al. Alzheimer's disease versus dementia with Lewy bodies: cerebral metabolic distinction with autopsy confirmation. Ann Neurol 2001;50:358–365.
32. Ishizawa T, Mattila P, Davies P, Wang D, Dickson DW. Colocalization of tau and alpha-synuclein epitopes in Lewy bodies. J Neuropathol Exp Neurol 2003;62:389–397.
33. Colom-Cadena M, Gelpi E, Charif S, et al. Confluence of alpha-synuclein, tau, and beta-amyloid pathologies in dementia with Lewy bodies. J Neuropathol Exp Neurol 2013;72:1203–1212.
34. Guo JL, Covell DJ, Daniels JP, et al. Distinct alpha-synuclein strains differentially promote tau inclusions in neurons. Cell 2013; 154:103–117.
35. Badiola N, de Oliveira RM, Herrera F, et al. Tau enhances alpha-synuclein aggregation and toxicity in cellular models of synucleinopathy. PLoS One 2011;6:e26609.
36. Giasson BI, Forman MS, Higuchi M, et al. Initiation and synergistic fibrillization of tau and alpha-synuclein. Science 2003;300:636–640.
37. Ferman TJ, Aoki N, Murray ME, et al. Disease trajectory and cognitive profiles of three pathologic subtypes of DLB. Am J Neurodegener Dis 2015;4(suppl 1):1–178.
38. Jack CR, Jr., Wiste HJ, Weigand SD, et al. Defining imaging biomarker cut points for brain aging and Alzheimer's disease. Alzheimers Dement 2016 Sep 30. pii: S1552-5260(16)32875-8. doi: 10.1016/j.jalz.2016.08.005. [Epub ahead of print]
39. Murray ME, Lowe VJ, Graff-Radford NR, et al. Clinicopathologic and ^{11}C-Pittsburgh compound B implications of Thal amyloid phase across the Alzheimer's disease spectrum. Brain 2015;138(pt 5):1370–1381.
40. Sarro L, Senjem ML, Lundt ES, et al. Amyloid-beta deposition and regional grey matter atrophy rates in dementia with Lewy bodies. Brain 2016;139(pt 10):2740–2750.
41. Whitwell JL, Weigand SD, Shiung MM, et al. Focal atrophy in dementia with Lewy bodies on MRI: a distinct pattern from Alzheimer's disease. Brain 2007;130(pt 3):708–719.
42. Nedelska Z, Ferman TJ, Boeve BF, et al. Pattern of brain atrophy rates in autopsy-confirmed dementia with Lewy bodies. Neurobiol Aging 2015;36:452–461.
43. Savica R, Grossardt BR, Bower JH, Ahlskog JE, Rocca WA. Incidence and pathology of synucleinopathies and tauopathies related to parkinsonism. JAMA Neurol 2013;70:859–866.
44. Imamura T, Ishii K, Hirono N, et al. Visual hallucinations and regional cerebral metabolism in dementia with Lewy bodies (DLB). Neuroreport 1999;10:1903–1907.
45. Kantarci K, Lowe VJ, Boeve BF, et al. Multimodality imaging characteristics of dementia with Lewy bodies. Neurobiol Aging 2012; 33:2091–2105.
46. Graff-Radford J, Lesnick T, Boeve BF, et al. Predicting survival in dementia with Lewy bodies with hippocampal volumetry. Am J Neurodegener Dis 2015;4(suppl 1):1–178.
47. Ballard CG, Jacoby R, Del Ser T, et al. Neuropathological substrates of psychiatric symptoms in prospectively studied patients with autopsy-confirmed dementia with lewy bodies. Am J psychiatry 2004;161:843–849.
48. Fujishiro H, Ferman TJ, Boeve BF, et al. Validation of the neuropathologic criteria of the third consortium for dementia with Lewy bodies for prospectively diagnosed cases. J Neuropathol Exp Neurol 2008;67:649–656.